Effect of Attenuation Correction on Lesion Detectability in FDG PET of Breast Cancer

Christian Bleckmann, Jörg Dose, Karl H. Bohuslavizki, Ralph Buchert, Susanne Klutmann, Janos Mester, Fritz Jänicke and Malte Clausen

Departments of Nuclear Medicine and Gynecology and Obstetrics, University Hospital Eppendorf, Hamburg, Germany

The aim of this study was to compare the visual analysis of attenuation-corrected and noncorrected ^{18}F-fluoro-2-deoxy-D-glucose (FDG) PET images in patients with primary or metastatic breast cancer using standardized film documentation and to evaluate the influence of attenuation correction on lesion detectability. **Methods:** Standard FDG PET of the breasts and of the axillary regions was performed on 28 women with breast cancer. Transmission scans were acquired for attenuation correction after administration of FDG. Transverse and coronal slices and maximum intensity projections both with and without attenuation correction were documented in a standardized manner on film. Noncorrected images were displayed with an upper threshold of five times the mean activity in normal lung tissue. Attenuation-corrected images were documented with an upper threshold of a standardized uptake value of five. Two independent nuclear medicine physicians, who were unaware of the results of clinical investigation, other imaging modalities and histopathologic findings, interpreted the images visually, noncorrected images first. **Results:** One hundred eighty-four of 189 lesions in 28 of 28 patients were found on attenuation-corrected and noncorrected images. Seventeen lesions were found in the breasts of 12 patients. In 18 patients, 31 axillary lesions were found. Moreover, 141 lesions representing distant metastases were detected in 18 patients. Attenuation-corrected images showed the same lesions in all patients but 2, in whom 5 of 189 small pulmonary lesions (2.6%) were not detected. Iterative reconstruction did not improve detectability of these lesions on attenuation-corrected images. These lesions were confirmed by CT, which revealed diameters of <1 cm. **Conclusion:** Attenuation correction by transmission measurement after injection may impair lesion detectability in PET for staging of breast cancer patients. When using the image modalities described, noncorrected PET images should be considered in image analysis.

Key Words: PET; breast cancer; attenuation correction; lesion detection

J Nucl Med 1999; 40:2021–2024

Breast cancer is the most common malignancy of women in the Western Hemisphere. The annual incidence in the United States between 1990 and 1995 was approximately 100 per 100,000 women (*1*). Almost 10% of women develop breast cancer during their lifetime. Early tumor detection and the presence of axillary lymph node metastases have been identified as the most important factors determining the prognosis of breast cancer patients (*2,3*). Mammography, MRI and sonography are common methods used for breast imaging (*4–9*). Although mammography and MRI provide a high sensitivity in the detection of breast cancer, their specificity is limited (*7*). Sonography may provide additional morphologic information (e.g., differentiation between cystic and solid tumors), whereas its specificity is low, similar to that of mammography (*6,9*). Increased uptake of ^{18}F-fluoro-2-deoxy-D-glucose (FDG) in breast cancer tissue was first reported in 1989 (*10,11*). In further studies, PET using FDG has shown both a high sensitivity and a high specificity in the detection of breast cancer. FDG PET allows the detection of multiple lesions and axillary lymph node involvement in primary breast cancer. The latter holds predominantly true for patients with locally advanced breast cancer (*12*). Although accurate staging of distant metastases conventionally requires several imaging modalities (i.e., radiography, sonography, CT or bone scanning), whole-body FDG PET may provide staging in one single procedure (*13*). Moreover, FDG PET may be useful as a prognostic indicator for breast cancer patients (*14–17*).

Most publications dealing with FDG PET in breast cancer are based on studies with attenuation correction (*13–26*). The main advantage of attenuation correction is an improved anatomic orientation (i.e., discrimination of lung tissue from liver or mediastinum). Moreover, using attenuation correction, images may be evaluated semiquantitatively (i.e., standardized uptake values [SUVs] can be calculated). The latter is important for therapy monitoring (*14–17*). A comparison of attenuation-corrected and noncorrected images in oncology has been obtained (*27*), including four patients with breast cancer. However, to our knowledge, the effect of attenuation correction on visual evaluation of FDG PET in breast cancer has not been determined on a broad basis.

Therefore, the aim of this study was to compare visual analysis of both attenuation-corrected and noncorrected FDG PET images in patients with primary or metastatic breast cancer using standardized film documentation.

Received Oct. 9, 1998; revision accepted Apr. 19, 1999.

For correspondence or reprints contact: Karl H. Bohuslavizki, MD, PhD, Department of Nuclear Medicine, University Hospital Eppendorf, Martinistr. 52, D-20246 Hamburg, Germany.

MATERIALS AND METHODS

Patients

Twenty-eight women with histologically proven breast cancer were investigated. Of these, 7 patients with newly diagnosed breast tumors were referred for FDG PET before surgery or neoadjuvant chemotherapy, and 21 women were referred for suspected relapse or distant metastases of breast cancer.

PET

Patients fasted for at least 6 h before PET to minimize blood insulin levels and glucose utilization of normal tissue (*28*). Before surgery, patients were imaged on a foam rubber support in the prone position with arms and breasts hanging freely. For the patients' comfort, investigations after surgery were performed in the supine position. Imaging was performed using an ECAT EXACT 47 scanner (CTI/Siemens, Inc., Knoxville, TN) (*29*). Emission scans of the breasts starting 40 min after intravenous administration of 350 MBq FDG and of axillary lymph nodes starting 50 min after injection were acquired for 10 min. Thereafter, transmission scanning was performed for 10 min per bed position using three rotating ^{68}Ge rod sources (*30,31*). Rod window settings were applied (i.e., all coincidences not passing through the current position of the rods were rejected). Rod window settings remove about 95% of scattered and random coincidences from the transmission measurement. In addition, rod window settings suppress by about the same percentage the emission contamination in transmission measurements after injection. No subtraction of the remaining emission counts was performed (*32*).

Documentation

Attenuation correction factors were obtained by dividing the sinogram data of a blank measurement (without the patient) acquired with the rod sources during the night by the sinogram data of the windowed transmission scan on a pixel-by-pixel basis (*33*). Scan duration and radioactive decay were taken into account. Attenuation-corrected emission data were reconstructed by filtered backprojection using a Hanning filter with a cutoff frequency of 0.4 of the Nyquist frequency. The transaxial spatial resolution was approximately 12 mm (full width at half maximum). PET images were printed on transparency film (Helios 810; Sterling Diagnostic Imaging, Bad Homburg, Germany) using a linear gray scale with the highest activity displayed in black. Noncorrected images were displayed with an upper threshold of five times the mean activity in the lung. Attenuation-corrected data were converted to SUVs and documented with an upper threshold of an SUV of five. SUVs were computed by normalizing the measured tumor radioactivity concentration to the injected dose and the total body mass (*34*). Differences in plasma glucose levels were neglected.

In selected patients, attenuation-corrected data were reconstructed iteratively by an ordered subset expectation maximization algorithm (*35*). This kind of algorithm has been shown to result in a significantly better signal-to-noise ratio with respect to tumors than filtered backprojection (*36*).

Standardized documentation on film included 20 transverse slices with a slice thickness of 13.5 mm, 20 coronal slices with a slice thickness of 13.5 mm and maximum-intensity projections in anterior, left lateral, right anterior oblique and left anterior oblique views as reported (*37*).

Image Analysis

Two independent nuclear medicine physicians, who were unaware of the results of clinical investigations, other imaging modalities and histopathologic findings, interpreted the images visually on a lesion-by-lesion basis. Lesions were graded 1–4 (1, definitely malignant; 2, high probability of malignancy; 3, low probability of malignancy; 4, definitely not malignant). Lesions graded as 1 or 2 were considered to be positive for malignancy. The same criteria were used for the noncorrected and the attenuation-corrected images. The subgroup of the noncorrected images was analyzed first. Interpretation of the attenuation-corrected images was performed independently in a different session, and images were read in different order. The observers reached consensus for each patient in both image-reading sessions. SUVs were calculated for image-scaling purposes only.

RESULTS

One hundred eighty-nine lesions were detected in 28 patients on noncorrected PET images. Twelve patients showed 17 lesions in their breasts. In 18 patients, 31 axillary lesions were found. Moreover, 141 lesions representing distant metastases were detected in liver, lung, bone and lymph nodes other than axillary in 18 patients. Coronal sections of a patient with small pulmonary lesions are shown in Figure 1.

Attenuation-corrected images showed the same lesions in all patients except 2 patients with multiple metastases, in whom 5 of 189 small pulmonary lesions (2.6%) were not detected (Fig. 1). Monitor analysis did not show the lesions either. Iterative reconstruction did not improve detectability of these lesions on attenuation-corrected images (Fig. 1). These lesions were confirmed by CT, which revealed diameters of <1 cm. The additional lesions detected on the noncorrected images did not lead to an upstaging of the patients' disease.

DISCUSSION

Sensitivity and specificity of FDG PET for detection of primary breast cancer vary from 68% to 96% and 78% to 100%, respectively (*21,23*). Accordingly, sensitivity and specificity for detection of axillary metastases vary from 70% to 100% and 67% to 100%, respectively (*12,19,24,25*). Sensitivity and specificity depend on the criteria used for image interpretation and on tumor size. Thus, FDG PET has been considered valuable for staging of breast cancer (*12,13,18,19,38*). Most studies that report on FDG PET in breast cancer are based on evaluation of attenuation-corrected images. The main advantages of attenuation correction are both an improved anatomic delineation and the ability to quantify tracer uptake. Although quantification may be helpful in several clinical settings (e.g., differentiation between benign and malignant tissue, treatment monitoring [*21,22*] and as a prognosis factor [*14*]), the necessity of attenuation correction has been questioned (*27*). Moreover, lesion detection is most important for accurate tumor staging, and it has been shown for several tumor entities (e.g., lymphoma or lung, colorectal or breast cancer) that quantification is not mandatory for this purpose (*27*). To our knowledge, lesion detection on attenuation-corrected im-

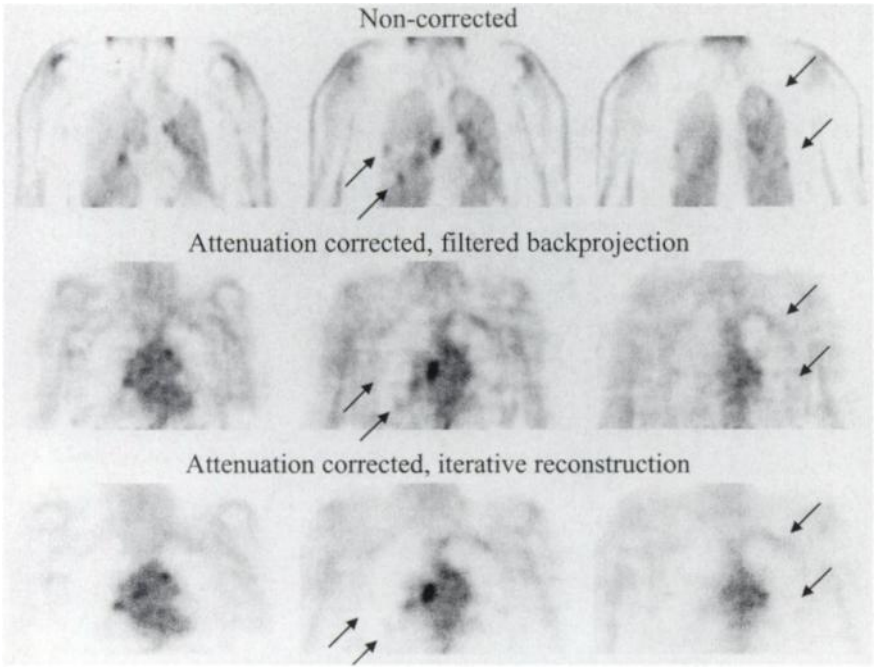

FIGURE 1. Coronal slices of FDG PET obtained in patient with multiple metastases of breast cancer. Pulmonary and mediastinal metastases are clearly visible on noncorrected images (top row). Four pulmonary metastases (arrows) are not seen on attenuation-corrected images reconstructed by filtered backprojection (middle row) or on images reconstructed iteratively (bottom row).

ages and on noncorrected images in breast cancer patients has not been compared systematically. Therefore, the aim of this study was to evaluate the effect of attenuation correction on lesion detection in routine clinical FDG PET in breast cancer.

In this study FDG PET images were documented on film in a standardized manner. The use of an appropriate threshold is of vital importance for lesion detection. Hence, establishing thresholds should be standardized to reduce both inter- and intraobserver variability. Attenuation-corrected images may be easily normalized with respect to quantitatively derived values (e.g., SUV). A range of SUV from zero to five has been established using PET in breast cancer (*21*). To normalize noncorrected images, we used normal lung tissue as an internal reference for tracer uptake. The upper threshold was set at five times mean activity in the lung (*37*). Although regional differences in FDG uptake in normal lung were described (*39*), variations were too small to be relevant in this context.

In this study, most lesions, i.e., 184 of 189 (97.4%), were detected on both image types, whereas only 5 of 189 lesions (2.6%) were not detected on attenuation-corrected images. This result agrees with the findings of a study comparing the regional tracer distribution on attenuation-corrected and noncorrected images of 34 patients undergoing FDG PET for tumor staging, including 4 patients with breast cancer (*27*). The tumor-to-background ratio was significantly higher on noncorrected images compared with attenuation-corrected images. Consequently, in most clinical situations attenuation correction may not be mandatory (*27*). A lower target-to-background ratio on attenuation-corrected images might be explained by several factors. First, measured transmission increases noise within reconstructed images (*40*). Second, because transmission scanning was performed after injection of FDG both to shorten the scanning time and to increase patient throughput, an increased activity within the tumor yields an artificially reduced tracer uptake within the lesion. Third, partial volume effects caused by patient movement, i.e., breathing, may lead to an underestimation of tracer uptake in small pulmonary lesions. On the basis of common experience, an increased noise might be overcome by prolonging acquisition time of transmission images. However, it was shown that contrast did not improve significantly when transmission duration was increased up to threefold (*27*). Moreover, noise in reconstructed images may be reduced by iterative reconstruction. Nevertheless, five pulmonary lesions were not detected on attenuation-corrected images reconstructed by filtered backprojection or on images generated by iterative reconstruction.

CONCLUSION

Attenuation correction by postinjection transmission measurement may impair lesion detectability in PET for staging of breast cancer. When using the image modalities described, noncorrected PET images should be considered in image analysis.

REFERENCES

1. Wingo PA, Ries LAG, Rosenberg HM, Miller DS, Edwards BK. Cancer incidence and mortality: 1973–1995. *Cancer.* 1998;82:1197–1207.
2. Chu KC, Smart CR, Tarone RE. Analysis of breast cancer mortality and stage distribution by age for the health insurance plan trial. *J Natl Cancer Inst.* 1988;80:1125–1132.
3. Carter CL, Allen C, Henson DE. Relation of tumor size, lymph node status, and survival in 24,740 breast cancer cases. *Cancer.* 1989;63:181–187.
4. Kopans DB, Meyer JE, Sadowsky N. Breast imaging. *N Engl J Med.* 1984;310:960–967.
5. Heywang SH, Wolf A, Pruss E, et al. MR imaging of the breast with Gd-DTPA: use and limitations. *Radiology.* 1989;171:95–103.

6. Egan RL, Egan KL. Detection of breast carcinoma: comparison of automated water-path whole-breast sonography, mammography, and physical examination. *AJR.* 1984;143:493–497.
7. Hermann G, Janus C, Schwartz IS, et al. Nonpalpable breast lesions: accuracy of prebiopsy mammographic diagnosis. *Radiology.* 1987;165:323–326.
8. Jackson VP. The role of ultrasound in breast imaging. *Radiology.* 1990;177:305–311.
9. Kacl GM, Liu P, Debatin JF, Garzoli E, Caduff RF, Krestin GP. Detection of breast cancer with conventional mammography and contrast-enhanced MR imaging. *Eur Radiol.* 1998;8:194–200.
10. Kubota K, Matsuzwana T, Amemiya A, et al. Imaging of breast cancer with (18-F) fluorodeoxyglucose and positron emission tomography. *J Comput Assist Tomogr.* 1989;13:1097–1098.
11. Minn H, Soini I. (18-F) fluorodeoxyglucose scintigraphy in the diagnosis and follow up of treatment in advanced breast cancer. *Eur J Nucl Med.* 1989;15:61–66.
12. Avril N, Dose J, Jänicke F, et al. Assessment of axillary lymph node involvement in breast cancer patients with positron emission tomography using radiolabeled 2-(fluorine-18)-fluoro-2-deoxy-D-glucose. *J Natl Cancer Inst.* 1996;88:1204–1209.
13. Moon DH, Maddahi J, Silverman DH, Glaspy JA, Phelps ME, Hoh CK. Accuracy of whole-body fluorine-18-FDG PET for the detection of recurrent or metastatic breast carcinoma. *J Nucl Med.* 1998;39:431–435.
14. Oshida M, Uno K, Suzuki M, et al. Predicting the prognoses of breast carcinoma patients with positron emission tomography using 2-deoxy-2-fluoro [^{18}F]-D-glucose. *Cancer.* 1998;82:2227–2234.
15. Jansson T, Westlin JE, Ahlström H, Lilja B, Langström B, Bergh J. Positron emission tomography studies in patients with locally advanced and/or metastatic breast cancer: a method for early therapy evaluation? *J Clin Oncol.* 1995;13:1470–1477.
16. Bassa P, Kim EE, Inoue T, et al. Evaluation of preoperative chemotherapy using PET with fluorine-18-fluorodeoxyglucose in breast cancer. *J Nucl Med.* 1996;37:931–938.
17. Wahl RL, Zasadny K, Helvie M, Hutchins GD, Weber B, Cody R. Metabolic monitoring of breast cancer chemohormonotherapy using positron emission tomography: initial evaluation. *J Clin Oncol.* 1993;11:2101–2111.
18. Noh DY, Yun IJ, Kim JS, et al. Diagnostic value of positron emission tomography for detecting breast cancer. *World J Surg.* 1998;22:223–227.
19. Crippa F, Agresti R, Seregni E, et al. Prospective evaluation of fluorine-18-FDG PET in presurgical staging of the axilla in breast cancer. *J Nucl Med.* 1998;39:4–8.
20. Nieweg OE, Kim EE, Wong WH, et al. Positron emission tomography with fluorine-18-deoxyglucose in the detection and staging of breast cancer. *Cancer.* 1993;71:3920–3925.
21. Avril N, Bense S, Ziegler SI, et al. Breast imaging with fluorine-18-FDG PET: quantitative image analysis. *J Nucl Med.* 1997;38:1186–1191.
22. Avril N, Dose J, Jänicke F, et al. Metabolic characterization of breast tumors with positron emission tomography using F-18-fluorodeoxyglucose. *J Clin Oncol.* 1996;14:1848–1857.
23. Adler LP, Crowe JP, Al-Kaisi NK, Sunshine JL. Evaluation of breast masses and axillary lymph nodes with [F-18] 2-deoxy-2-fluoro-D-glucose PET. *Radiology.* 1993;187:743–750.
24. Adler LP, Faulhaber PF, Schnur KC, Al-Kasi NL, Shenk RR. Axillary lymph node metastases: screening with [F-18] 2-deoxy-2-fluoro-D-glucose (FDG) PET. *Radiology.* 1997;203:323–327.
25. Utech CI, Young CS, Winter PF. Prospective evaluation of fluorine-18 fluorodeoxyglucose positron emission tomography in breast cancer for staging of the axilla related to surgery and immunocytochemistry. *Eur J Nucl Med.* 1996;23:1588–1593.
26. Wahl RL, Cody RL, Hutchins GD, Mudgett EE. Primary and metastatic breast carcinoma: initial clinical evaluation with PET with the radiolabeled glucose analogue 2-[F-18]-fluoro-2-deoxy-D-glucose. *Radiology.* 1991;179:765–770.
27. Bengel FM, Ziegler SI, Avril N, Weber W, Laubenbacher C, Schwaiger M. Whole-body positron emission tomography in clinical oncology: comparison between attenuation-corrected and uncorrected images. *Eur J Nucl Med.* 1997;24:1091–1098.
28. Minn H, Leskinen-Kallio S, Lindholm P, et al. (18-F) fluorodeoxyglucose uptake in tumors: kinetic vs. steady-state methods with reference to plasma insulin. *J Comput Assist Tomogr.* 1993;17:115–123.
29. Wienhard K, Eriksson L, Grootoonk S, Casey ME, Pietrzyk U, Heiss WD. Performance evaluation of the positron scanner ECAT EXACT. *J Comput Assist Tomogr.* 1992;16:804–813.
30. Carroll LR, Kretz P, Orcutt G. The orbiting rod source: improving performance in PET transmission correction scans. In: Esser PD, ed. *Emission Computed Tomography: Current Trends.* New York, NY: Society of Nuclear Medicine; 1983:235–247.
31. Carson RE, Daube-Witherspoon ME, Green MV. A method for postinjection PET transmission measurements with a rotating source. *J Nucl Med.* 1988;29:1558–1567.
32. Schulz G, Ostwald E, Schreckenberger M, et al. Attenuation corrected myocardial PET using post injection transmission measurement: influence on relative regional uptake values. *Nuklearmedizin.* 1998;37:166–170.
33. Ostertag H, Kübler WK, Doll J, Lorenz W. Measured attenuation correction methods. *Eur J Nucl Med.* 1989;15:722–726.
34. Zasadny K, Wahl RL. Standardized uptake values of normal tissues at PET with 2-[fluorine-18]-fluoro-2-deoxy-D-glucose: variations with body weight and a method for correction. *Radiology.* 1993;189:847–850.
35. Hudson HM, Larkin RS. Accelerated image reconstruction using ordered subsets of projection data. *IEEE Trans Med Imaging.* 1994;13:601–609.
36. Meikle SR, Hutton BF, Baily DL, Hooper PK, Fulham MJ. Accelerated EM reconstruction in total body PET: potential for improving tumour detectability. *Phys Med Biol.* 1994;39:1689–1704.
37. Bleckmann C, Buchert R, Schulte U, et al. Onco-PET: lesion detection by computer display versus standardized documentation on film. *Nuklearmedizin.* 1999;38:56–60.
38. Wahl RL. Overview of the current status of PET in breast cancer imaging. *Q J Nucl Med.* 1998;42:1–7.
39. Miyauchi T, Wahl R. Regional 2-[^{18}F]fluoro-2-deoxy-D-glucose uptake varies in normal lung. *Eur J Nucl Med.* 1996;23:517–523.
40. Huang SC, Hoffman EJ, Phelps ME, Kuhl DE. Quantification in positron emission computed tomography: effects of inaccurate attenuation correction. *J Comput Assist Tomogr.* 1979;3:804–814.